Ill-Defined Topological Phases in Local Dispersive Photonic Crystals

Filipa R. Prudêncio[1,2,*] and Mário G. Silveirinha[1]
[1]University of Lisbon–Instituto Superior Técnico and Instituto de Telecomunicações, Avenida Rovisco Pais 1, 1049-001 Lisbon, Portugal
[2]Instituto Universitário de Lisboa (ISCTE-IUL), Avenida das Forças Armadas 376, 1600-077 Lisbon, Portugal

(Received 7 December 2021; accepted 19 August 2022; published 23 September 2022)

In recent years there has been a great interest in topological materials and in their fascinating properties. Topological band theory was initially developed for condensed matter systems, but it can be readily applied to arbitrary wave platforms with few modifications. Thus, the topological classification of optical systems is usually regarded as being mathematically equivalent to that of condensed matter systems. Surprisingly, here we find that both the particle-hole symmetry and the dispersive nature of nonreciprocal photonic materials may lead to situations where the usual topological methods break down and the Chern topology becomes ill defined. It is shown that due to the divergence of the density of photonic states in plasmonic systems the gap Chern numbers can be noninteger notwithstanding that the relevant parametric space is compact. In order that the topology of a dispersive photonic crystal is well defined, it is essential to take into account the nonlocal effects in the bulk materials. We propose two different regularization methods to fix the encountered problems. Our results highlight that the regularized topologies may depend critically on the response of the bulk materials for large $\mathbf{k}$.

DOI: 10.1103/PhysRevLett.129.133903

Topological concepts have created exciting opportunities and unveiled hidden connections between different branches of physics, ranging from condensed matter to photonics [1–12]. In particular, in the case of optics, topological ideas have offered a more profound understanding of the wave propagation in nonreciprocal platforms, through the link between the topological charge of a medium and the emergence of edge states at the boundaries [13–16].

While the topological band theory was initially developed for condensed matter systems, the theory can be extended with few modifications to nearly arbitrary wave platforms, independent of the nature (fermionic or bosonic) of the system. In fact, the calculation of topological invariants in physical systems can very often be reduced to the problem of characterizing the topology of a two-parameter family of differential (possibly non-Hermitian) linear operators [17]. Apart from a few technical aspects related to the material dispersion [6,7,18], the topological band theory of photonic systems is usually regarded as being essentially equivalent to its condensed matter counterpart, with the main differences arising from the physical manifestations of the topology in fluctuation-induced phenomena (e.g., [16,19,20]).

The objective of this Letter is to highlight that the material dispersion and the particle-hole symmetry specific of bosonic systems may lead to rather peculiar situations where the standard topological methods break down and the Chern topology becomes ill defined. We find that in order to ensure that the topology of a dispersive photonic crystal is well defined it is absolutely essential to take into account the spatially dispersive response (i.e., dependence of the permittivity on the wave vector) of the bulk materials. In particular, our results demonstrate that rather surprisingly the cutoff associated with the spatial periodicity of photonic crystals is insufficient to guarantee a well-defined topology.

In order to illustrate the ideas, we consider a 2D photonic crystal formed by a hexagonal array of air rods embedded in an electric gyrotropic host [inset of Fig. 1(b)(i)]. The gyrotropic material is described by a permittivity tensor of the form $\bar{\varepsilon}_{\rm loc} = \varepsilon_t \mathbf{1}_t + i\varepsilon_g \hat{\mathbf{z}} \times \mathbf{1}_t + \varepsilon_a \hat{\mathbf{z}} \otimes \hat{\mathbf{z}}$, with $\varepsilon_t = 1 - [\omega_p^2/(\omega^2 - \omega_c^2)]$, $\varepsilon_g = (1/\omega)[\omega_p^2 \omega_c/(\omega_c^2 - \omega^2)]$, and $\varepsilon_a = 1 - (\omega_p^2/\omega^2)$. Here, $\omega_c = -qB_0/m$ is the cyclotron frequency, $q = -e$ is the elementary charge, m is the effective mass, $\mathbf{B}_0 = B_0 \hat{\mathbf{z}}$ is the bias magnetic field, and ω_p is the plasma frequency. The operators $\times$ and $\otimes$ represent the cross and the tensor products, respectively, and $\mathbf{1}_t = \hat{\mathbf{x}} \otimes \hat{\mathbf{x}} + \hat{\mathbf{y}} \otimes \hat{\mathbf{y}}$. The sign of ω_c depends on the orientation of the bias magnetic field B_0. The magnetic response is assumed trivial ($\mu = \mu_0$). Similar material responses occur naturally in magnetically biased semiconductors, e.g., InSb [21,22].

It is well known that the continuous translational symmetry of the bulk medium causes its topology to be ill defined [18]. It is common understanding that the creation of a crystalline structure, e.g., with a periodic array of inclusions in a host medium, effectively regularizes

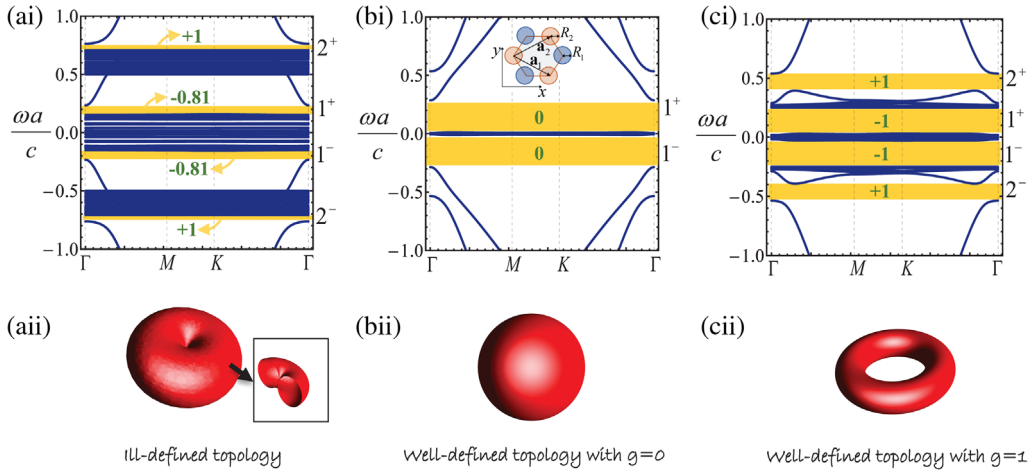

FIG. 1. Top row: photonic band structures of dispersive photonic crystals formed by a hexagonal array of air rods embedded in a magnetized electric plasma (geometry of the unit cell is sketched in the inset of panel (b)(i). The radius of the rods is $R_1 = R_2 = 0.4a$. The nearest neighbors distance is $a = 0.5c/\omega_p$. Each scalar component of the state vector is expanded with 49 plane waves. The green insets give the numerically calculated gap Chern numbers. The dispersive host material is characterized by (a) local model with $\omega_c = \omega_p$, (b) hydrodynamic model with $\omega_c = 0.5\omega_p$ and $\beta = 0.5c$, and (c) full cutoff model with $\omega_c = 0.5\omega_p$ and $k_{\max} = 2\omega_p/c$. Bottom row: geometrical illustration of the concepts of ill-defined topology and topology regularization. A torus with a vanishing inner radius [panel (a)] has an ill-defined topology because the surface is not differentiable at the central point where the adjoining top and bottom sections touch at a single point (cusp). By either separating the top and bottom sections of the surface [panel (b) showing a sphere] or by opening a hole in the central region [panel (c) showing a torus] one can regularize the topology of the original object. Similar to the electric gyrotropic plasma, the topology of the regularized object depends on the regularization procedure.

the topology of the system because it leads to a compact parametric space: the first Brillouin zone (BZ). Note that in the continuous case the parametric space is the Euclidean plane, which is not compact [18]. It is worth mentioning that the calculation of topological invariants of photonic crystals is a rather formidable problem from a computational point of view, and to our best knowledge the characterization of the topology of dispersive photonic crystals was not reported in the literature. Up to now, only a few works studied the topology of photonic crystals using first principles methods [8,23,24], but the material dispersion was always ignored.

Figure 1(a)(i) shows the band structure of a representative dispersive photonic crystal geometry, showing both positive and negative frequencies. The band structure is numerically computed using the plane wave method [25]. To this end, the spectral problem must be first formulated as a standard eigenvalue problem of the type $\hat{L}_{\mathbf{k}} \cdot \mathbf{Q}_{n\mathbf{k}} = E_{n\mathbf{k}}\mathbf{Q}_{n\mathbf{k}}$, with $E_{n\mathbf{k}} = \omega_{n\mathbf{k}}/c$ and $\hat{L}_{\mathbf{k}}$ a differential operator independent of the frequency. Typically, this entails modeling the effects of the material dispersion with additional variables that represent the internal degrees of freedom of the medium responsible for the dispersive response [18,26,27]. Here, the relevant state vector $\mathbf{Q}_{n\mathbf{k}}$ is formed not only by the electromagnetic fields but also by the current density and charge density in the magnetized plasma [28].

Because of the reality of the electromagnetic field (bosonic field), the spectrum is constrained by the particle-hole symmetry $\omega(\mathbf{k}) = -\omega(-\mathbf{k})$, which implies that the positive frequency and negative frequency spectra are linked by a mirror symmetry, consistent with Fig. 1(a)(i). As seen, there are two complete gaps with positive frequency, and evidently two complete gaps with negative frequency. Furthermore, due to the dispersive nature of the material response, one sees an accumulation of an infinite number of branches for both very low frequencies and for frequencies on the order of ω_p. This property is rooted in the plasmonic-gyrotropic material response, which originates localized resonances that hybridize to form quasiflat bands. A similar effect has been previously reported in reciprocal metallic photonic crystals [29,30].

The topology of the photonic crystal is characterized with the system Green's function $G_{\mathbf{k}}(\omega) = i(\hat{L}_{\mathbf{k}} - \mathbf{1}\omega)^{-1}$ [17,24,31,32]. The operator $\hat{L}_{\mathbf{k}}$ is parametrized by the real wave vector $\mathbf{k} = k_x\hat{\mathbf{x}} + k_y\hat{\mathbf{y}}$ that determines the Bloch-type boundary conditions in a unit cell. The poles of the Green's function coincide with the eigenfrequencies $\omega = \omega_{n\mathbf{k}}$ of $\hat{L}_{\mathbf{k}}$. The eigenfrequencies are separated in the complex plane by vertical strips that determine the band gaps (in the lossless case the eigenfrequencies lie in the real axis; in the non-Hermitian case they may populate other parts of the complex plane, $\omega = \omega' + i\omega''$) [17,24]. The gap Chern number of each spectral band gap can be expressed in terms of the Green's function through an integral in the complex plane over a line contained in the band gap ($\omega = \omega_{\text{gap}} + i\omega''$ with $-\infty < \omega'' < \infty$):

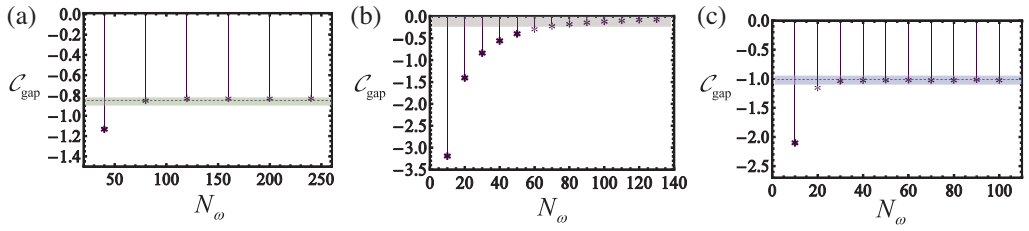

FIG. 2. Convergence study of the numerically calculated (positive low-frequency, 1^+) gap Chern number $C_{\rm gap}$ for a photonic crystal described by (a) the local model (b) the hydrodynamic model and (c) the full cutoff model. The photonic crystal parameters are as in Fig. 1. The integral in the complex frequency plane is evaluated with N_ω sampling points, shown in the horizontal axis of the plots. In all the simulations, each scalar component of the state vector is expanded with 49 plane waves ($n_{\rm max} = 3$) and each direction of the BZ is sampled with $N = 20$ points.

$$C_{\rm gap} = \frac{i}{(2\pi)^2} \iint_{\rm BZ} d^2\mathbf{k} \int_{E_{\rm gap}-i\infty}^{E_{\rm gap}+i\infty} dE\, {\rm Tr}\{\partial_1 \hat{L}_{\mathbf{k}} \cdot G_{\mathbf{k}} \cdot \partial_2 \hat{L}_{\mathbf{k}} \cdot G_{\mathbf{k}}^2\}. \tag{1}$$

Here, ${\rm Tr}\{\cdots\}$ is the trace operator, $\partial_j = \partial/\partial k_j$ ($j = 1, 2$) with $k_1 = k_x$ and $k_2 = k_y$, $E_{\rm gap} = \omega_{\rm gap}/c$ is some normalized (real-valued) frequency in the gap [17,24,31], and the integral in $\mathbf{k}$ is over the BZ. The relevant differential operators and the Green's function are represented by matrices in a plane wave basis [28]. The topological classification with the Green's function does not require knowledge of the eigenfunctions (Bloch modes) of the photonic crystal [18,31].

The Green's function method determines directly the gap Chern number, i.e., the sum of all Chern numbers below the gap. In our understanding, this is only method that can be applied to compute the topological charge of a dispersive photonic crystal. In fact, typically there is an infinite number of bands below the gap and thereby it is impracticable to apply the standard topological band theory, as that would require evaluating separately the individual contributions of all bands below the gap. The situation is particularly acute in the dispersive case due to the accumulation of an infinite number of branches at finite frequencies, as illustrated in Fig. 1(a)(i).

Figure 2(a) reports a convergence study of the low-frequency gap Chern number. A more complete analysis can be found in Supplemental Material [28], including the effect of material dissipation. Puzzlingly, we find that the low-frequency gap Chern number of the dispersive photonic crystal is not an integer: the converged numerical calculations yield $C_{\rm gap}^{1+} \approx -0.81$. The value of $C_{\rm gap}^{1+}$ is sensitive to perturbations of the structural parameters [28]. On the other hand, for the positive high-frequency gap the converged Chern number is $C_{\rm gap}^{2+} = 1$, which as expected is an integer and is insensitive to perturbations of the geometry or to dissipation effects that do not close the gap [28]. The ill-defined topology of the low-frequency gap seemingly contradicts the Chern theorem, which naively is expected to apply because the parametric space (BZ) is a compact set with no boundary. In the following, we argue that the topology may be ill defined due to two reasons: (i) the existence of an infinite number of bands below the gap, and (ii) the accumulation of an infinite number of branches at a single frequency. The latter reason is the relevant one for the system under analysis.

As previously noted, photonic systems are constrained by the particle-hole symmetry. Then, different from electronic systems which have a well-defined "ground," in the photonic case it is possible to have an infinite number of bands below a band gap. Indeed, the number of bands with negative frequency is typically infinite. There is a widespread belief that the total topological charge of negative frequency bands vanishes, and so they do not play any role. Such an understanding is flawed: for a counterexample in a system with a continuous translational symmetry, i.e., an electromagnetic continuum, see Ref. [16]. Below we also present a counterexample in a photonic crystal. In fact, the particle-hole symmetry only implies that the total topological charge of positive frequency bands has the opposite sign of the charge of negative frequency bands, nothing more.

The potential problem of having an infinite number of bands below the gap is illustrated in Fig. 3(a). Consider the band gap shaded in yellow. As the corresponding gap Chern number is given by $C_{\rm gap} = \delta C_1 + \delta C_2 + \cdots$, with δC_i the Chern numbers of the bands below the gap, it follows that $C_{\rm gap}$ is given by an infinite sum of integers. In general, such a series is divergent. For example, suppose that $\delta C_i = (-1)^i$. Then, the gap Chern number is given by $C_{\rm gap} = -1 + 1 - 1 + \cdots$, which is evidently not convergent in the usual sense. In fact, a series of the type $C_{\rm gap} = \delta C_1 + \delta C_2 + \cdots$ with δC_i integer can converge only when the number of nonvanishing terms is finite. Fortunately, there is a relatively simple way to ensure the series convergence. Intuitively, provided the response of the nonreciprocal materials approaches that of the vacuum ($\bar{\varepsilon} \to \varepsilon_0 \mathbf{1}$) when $\omega \to \infty$, the topological charge of bands with large frequency is expected to be trivial (i.e., $\delta C_i = 0$) for a sufficiently large i. Note that the constraint $\bar{\varepsilon}_{\omega\to\infty} \to \varepsilon_0 \mathbf{1}$ is consistent with the Kramers-Kronig

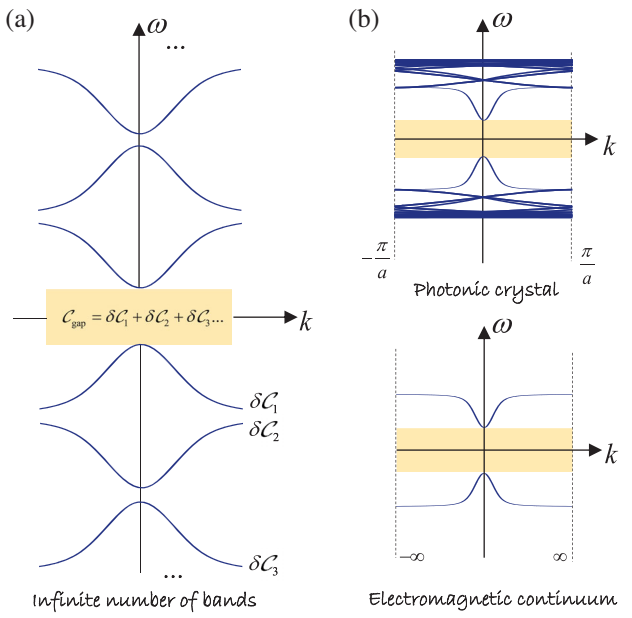

FIG. 3. (a) Illustration of the band structure of a generic photonic crystal. Because of the particle-hole symmetry the gap Chern number is generally given by an infinite sum of integers, corresponding to the sum of the Chern numbers of all the bands below the gap. (b) The accumulation of branches at a single frequency in a gyrotropic photonic crystal (top panel, with the wave vector restricted to the BZ) may be regarded as a consequence of the band folding of the dispersion of the bulk material (bottom panel, with the wave vector range unconstrained).

formulas [33], and is satisfied by the dispersive model considered here.

Importantly, another convergence issue may arise even when the physical constraint $\bar{\varepsilon}_{\omega\to\infty} \to \varepsilon_0\mathbf{1}$ is satisfied. In fact, suppose that a certain band is formed by an infinite number of "branches," i.e., that there is an accumulation of eigenvalues at a finite frequency [see Fig. 3(b), top panel]. Intuitively, the Chern number δC of the band is a sum of an infinite number of integer contributions, resulting in an ill-defined topology for the same reasons as before. A more rigorous argument is developed in Supplemental Material [28]. The described situation is precisely what happens in Fig. 1(a)(i): the topological charge of the band in between gaps 1^+ and 2^+ is given by $\delta C = C^{2+}_{\text{gap}} - C^{1+}_{\text{gap}} = 1.81$. In contrast, the topological charge of all the bands above gap 2^+ is $\delta C = 0 - C^{2+}_{\text{gap}} = -1$; the topology of these bands is well defined because above gap 2^+ there are no plasmonic-type localized resonances, and thereby there is no accumulation of eigenvalues at a finite frequency.

The problem identified in the previous paragraph can be fixed in two ways. The first solution is to guarantee that there is no accumulation of branches at a finite frequency. For the particular system under study, this can be done taking into account the effects of charge diffusion in the electron gas using the so-called "hydrodynamic" model [22,34–37]. The strength of the diffusion term is determined by the velocity β, which typically corresponds to the velocity of electrons at the Fermi level. The physical origin of the diffusion term is the electron-electron repulsive interactions. Figure 1(b)(i) shows the photonic band structure of a dispersive photonic crystal, with the diffusion effects modeled by $\beta = 0.5c$ (this unrealistically large value of β is chosen to have larger gaps and speed up the numerical calculations; the topology of the gap 1^+ is independent of the value of $\beta > 0$). As seen, a nonzero value of β may change considerably the band structure as compared to the local model of Fig. 1(a)(i). Now, there is a single positive-frequency band gap determined by $0.01 < \omega c/a < 0.29$. This band gap remains open if β is decreased continuously down to zero (see Ref. [28]), and hence it can be identified with the gap 1^+ of the local model. As seen in Fig. 1(b)(i), the diffusion effects prevent the accumulation of bands at a single frequency. In agreement with this property, we find that the gap Chern number is now an integer, $C^{1+}_{\text{gap}} = 0$, and thereby the dispersive photonic crystal has a trivial topology. The convergence analysis is reported in Fig. 2(b) and in [28].

Next, we discuss a second and more general solution to regularize the topology of the dispersive photonic crystal. To begin with, we note that the accumulation of branches at a single frequency can be regarded as a consequence of the band folding of the dispersion of the bulk-host material [Fig. 3(b)]. From this point of view, the ill-defined topology of the photonic crystal is inherited from the ill-defined topology of the host material [18]. This suggests that a regularization of the topology of the host material may also fix the topology of the photonic crystal. Reference [18] introduced a general solution to regularize the topology of an electromagnetic continuum; the procedure is based on the introduction of a full spatial cutoff k_{max} that guarantees that $\bar{\varepsilon}_{\mathbf{k}\to\infty} \to \varepsilon_0\mathbf{1}$. In other words, the material response is suppressed for large wave vectors so that it becomes identical to that of free space. This can be implemented by modifying the original local response ($\bar{\varepsilon}_{\text{loc}}$) in such a way that $\bar{\varepsilon}_{\text{nonloc}} = \varepsilon_0\mathbf{1} + [1/(1 + k^2/k^2_{\text{max}})](\bar{\varepsilon}_{\text{loc}} - \varepsilon_0\mathbf{1})$ [18]. Note that for values of $k \ll k_{\text{max}}$ the cutoff leaves the original response almost unchanged. It is relevant to underline that the constraint $\bar{\varepsilon}_{\mathbf{k}\to\infty} \to \varepsilon_0\mathbf{1}$ is rather physical, as it is a necessary consequence of the Kramers-Kronig relations for media with spatial dispersion and of the Riemann-Lebesgue lemma [33,38]. Figure 1(c)(i) reports the band structure of a dispersive photonic crystal with the spatial cutoff $k_{\text{max}} = 2\omega_p/c$. The relevant formalism and the details of the numerical implementation are given in [28]. Different from the hydrodynamic model, the two original band gaps are now preserved as they remain open when the cutoff is introduced [28]. Moreover, different from the hydrodynamic model, there is still an accumulation of branches at a single frequency. However, the numerical calculations reveal that the topology of the

two band gaps is well defined, yielding $C_{\mathrm{gap}}^{2+}=1$ and $C_{\mathrm{gap}}^{1+}=-1$ [see Fig. 2(c) and [28] for the convergence analysis and for the explanation why the cutoff k_{max} regularizes the topology]. In particular, this example nicely illustrates that the total topological charge of the negative frequency bands can be nontrivial as $C_{\mathrm{gap}}^{1-}\neq 0$.

Remarkably, even though both the hydrodynamic and the full cutoff models regularize the topology of the gap 1^+ of the original problem, they lead to a different gap Chern number. This property can be explained in a geometrical way (see the bottom row of Fig. 1). The original (local) dispersive photonic crystal may be regarded as the counterpart of a nondifferentiable geometric surface, e.g., a torus with vanishing inner radius as shown in Fig. 1(a)(ii). As the topology of a geometric surface is determined by the number of holes (genus), the topology of a torus with vanishing radius is ill defined because the top and bottom sections touch at exactly one point. The surface topology can be regularized with a negligibly weak perturbation of the original shape. One option is to separate the top and bottom sections to obtain an object topologically equivalent to a sphere [Fig. 1(b)(ii)]. Another option is to insert a hole in the middle region to create a torus with a nonzero inner radius [Fig. 1(c)(ii)]. Evidently, the topology of the two regularized objects (the genus) is different. In fact, it depends on the regularization procedure, in the same manner as the topology of the regularized photonic crystal depends if one adopts the hydrodynamic model or the full cutoff model. For a physical system the regularization is not arbitrary: it depends on the microscopic processes that determine the nonlocality.

In summary, it was shown that surprisingly the periodicity of a dispersive (and possibly lossy) photonic crystal does not guarantee a well-defined topology. It was highlighted that both the particle-hole symmetry and the accumulation of resonances at a single frequency (e.g., divergence of the density of photonic states due to plasmonic resonances and band folding) can lead to ill-defined topologies, where the gap Chern number is not an integer. We proposed two solutions to fix the encountered problem. The first solution exploits charge diffusion to prevent the accumulation of bands at a single frequency; the second solution, which is applicable in any scenario, ensures that the contribution of most branches is trivial by suppressing the material response for large wave vectors. An important corollary of our findings is that the topology of any dispersive photonic crystal generally depends critically on the high-spatial frequency response of the involved bulk materials. Thus, the number of topological edge states may be predicted only with a detailed knowledge of the microscopic mechanisms that determine the nonlocal response of the bulk materials. To conclude, we observe that nonreciprocal systems with ill-defined topologies are interesting on their own [39–43], as they may enable the emergence of topological energy sinks that can be useful for energy harvesting [39].

This work is supported in part by the IET under the A. F. Harvey Engineering Research Prize, by the Simons Foundation under Award No. 733700 (Simons Collaboration in Mathematics and Physics, "Harnessing Universal Symmetry Concepts for Extreme Wave Phenomena"), and by Fundação para a Ciência e a Tecnologia and Instituto de Telecomunicações under Project No. UID/EEA/50008/2020.

*Corresponding author.
filipa.prudencio@lx.it.pt

[1] D. J. Thouless, M. Kohmoto, M. P. Nightingale, and M. den Nijs, Quantized Hall Conductance in a Two-Dimensional Periodic Potential, Phys. Rev. Lett. **49**, 405 (1982).
[2] F. D. M. Haldane, Model for a Quantum Hall Effect without Landau Levels: Condensed-Matter Realization of the Parity Anomaly, Phys. Rev. Lett. **61**, 2015 (1988).
[3] C. L. Kane and E. J. Mele, Z_2 Topological Order and the Quantum Spin Hall Effect, Phys. Rev. Lett. **95**, 146802 (2005).
[4] M. Z. Hasan and C. L. Kane, Colloquium: Topological insulators, Rev. Mod. Phys. **82**, 3045 (2010).
[5] M. C. Rechtsman, J. M. Zeuner, Y. Plotnik, Y. Lumer, D. Podolsky, F. Dreisow, S. Nolte, M. Segev, and A. Szameit, Photonic Floquet topological insulators, Nature (London) **496**, 196 (2013).
[6] S. Raghu and F. D. M. Haldane, Analogs of quantum-Hall-effect edge states in photonic crystals, Phys. Rev. A **78**, 033834 (2008).
[7] F. D. M. Haldane and S. Raghu, Possible Realization of Directional Optical Waveguides in Photonic Crystals with Broken Time-Reversal Symmetry, Phys. Rev. Lett. **100**, 013904 (2008).
[8] Z. Wang, Y. Chong, J. D. Joannopoulos, and M. Soljačić, Observation of unidirectional backscattering immune topological electromagnetic states, Nature (London) **461**, 772 (2009).
[9] A. B. Khanikaev, S. H. Mousavi, W. K. Tse, M. Kargarian, A. H. MacDonald, and G. Shvets, Photonic topological insulators, Nat. Mater. **12**, 233 (2012).
[10] S. Lannebère and M. G. Silveirinha, Photonic analogues of the Haldane and Kane-Mele models, Nanophotonics **8**, 1387 (2019).
[11] L. Lu, J. D. Joannopoulos, and M. Soljacic, Topological photonics, Nat. Photonics **8**, 821 (2014).
[12] T. Ozawa, H. M. Price, A. Amo, N. Goldman, M. Hafezi, L. Lu, M. C. Rechtsman, D. Schuster, J. Simon, O. Zilberberg, and I. Carusotto, Topological Photonics, Rev. Mod. Phys. **91**, 015006 (2019).
[13] Y. Hatsugai, Chern Number and Edge States in the Integer Quantum Hall Effect, Phys. Rev. Lett. **71**, 3697 (1993).
[14] A. M. Essin and V. Gurarie, Bulk-boundary correspondence of topological insulators from their respective Green's functions, Phys. Rev. B **84**, 125132 (2011).

[15] M. G. Silveirinha, Bulk edge correspondence for topological photonic continua, Phys. Rev. B **94**, 205105 (2016).
[16] M. G. Silveirinha, Proof of the Bulk-Edge Correspondence through a Link between Topological Photonics and Fluctuation-Electrodynamics, Phys. Rev. X **9**, 011037 (2019).
[17] M. G. Silveirinha, Topological theory of non-Hermitian photonic systems, Phys. Rev. B **99**, 125155 (2019).
[18] M. G. Silveirinha, Chern invariants for continuous media, Phys. Rev. B **92**, 125153 (2015).
[19] M. G. Silveirinha, Topological angular momentum and radiative heat transport in closed orbits, Phys. Rev. B **95**, 115103 (2017).
[20] M. G. Silveirinha, Quantized angular momentum in topological optical systems, Nat. Commun. **10**, 349 (2019).
[21] E. Palik, R. Kaplan, R. Gammon, H. Kaplan, R. Wallis, and J. Quinn, Coupled surface magnetoplasmon-optic phonon polariton modes on InSb, Phys. Rev. B **13**, 2497 (1976).
[22] J. A. Bittencourt, *Fundamentals of Plasma Physics*, 3rd ed. (Springer-Verlag, New York, 2010).
[23] R. Zhao, G. Xie, M. L. N. Chen, Z. Lan, Z. Huang, and W. E. I. Sha, First-principle calculation of Chern number in gyrotropic photonic crystals, Opt. Express **28**, 380077 (2020).
[24] F. R. Prudêncio and M. G. Silveirinha, First principles calculation of topological invariants of non-Hermitian photonic crystals, Commun. Phys. **3**, 221 (2020).
[25] K. Sakoda, *Optical Properties of Photonic Crystals* (Springer, Berlin 2001).
[26] A. Raman and S. Fan, Photonic Band Structure of Dispersive Metamaterials Formulated as a Hermitian Eigenvalue Problem, Phys. Rev. Lett. **104**, 087401 (2010).
[27] M. G. Silveirinha, Modal expansions in dispersive material systems with application to quantum optics and topological photonics, in *Advances in Mathematical Methods for Electromagnetics*, edited by Paul Smith and Kazuya Kobayashi (Scitech Publishing, IET, 2021).
[28] See Supplemental Material at http://link.aps.org/supplemental/10.1103/PhysRevLett.129.133903 with (a) Formulation of the spectral problems as standard eigenvalue problems. (b) Representation of the operator $\hat{L}_{\mathbf{k}}$ in a plane wave basis. (c) Continuous evolution of the band diagrams of the hydrodynamic and full cutoff models to the band diagram of the local model. (d) Numerical study of the convergence of the gap Chern numbers and effect of material dissipation. (e) The origin of the ill-defined Chern number.
[29] A. R. McGurn and A. A. Maradudin, Photonic band structures of two- and three-dimensional periodic metal or semiconductor arrays, Phys. Rev. B **48**, 17576 (1993).
[30] V. Kuzmiak, A. A. Maradudin, and F. Pincemin, Photonic band structures of two-dimensional systems containing metallic components, Phys. Rev. B **50**, 16835 (1994).
[31] M. G. Silveirinha, Topological classification of Chern-type insulators of the photonic Green function, Phys. Rev. B **97**, 115146 (2018).
[32] B. A. Bernervig and T. Hughes, *Topological Insulators and Topological Superconductors* (Princeton University Press, Princeton, NJ, 2013).
[33] L. D. Landau, L. P. Pitaevskii, and E. M. Lifshitz, *Electrodynamics of Continuous Media* (Elsevier Science & Technology, United Kingdom, 1984), Vol. 8.
[34] S. Raza, S. I. Bozhevolnyi, M. Wubs, and N. A. Mortensen, Nonlocal optical response in metallic nanostructures, J. Phys. Condens. Matter **27**, 183204 (2015).
[35] S. V. Silva, T. A. Morgado, and M. G. Silveirinha, Multiple embedded eigenstates in nonlocal plasmonic nanostructures, Phys. Rev. B **101**, 041106(R) (2020).
[36] S. Gangarai and F. Monticone, Do truly unidirectional surface plasmon-polaritons exist?, Optica **6**, 1158 (2019).
[37] S. Buddhiraju, Y. Shi, A. Song, C. Wojcik, M. Minkov, I. A. D. Williamson, A. Dutt, and S. Fan, Absence of unidirectionally propagating surface plasmon-polaritons in nonreciprocal plasmonics, Nat. Commun. **11**, 674 (2020).
[38] V. Agranovich and V. Ginzburg, *Spatial Dispersion in Crystal Optics and the Theory of Excitons* (Wiley-Interscience, New York, 1966).
[39] D. E. Fernandes and M. G. Silveirinha, Topological Origin of Electromagnetic Energy Sinks, Phys. Rev. Applied **12**, 014021 (2019).
[40] A. Ishimaru, Unidirectional waves in anisotropic media and the resolution of the thermodynamic paradox, Technical Report 69, US Air Force, 1962.
[41] U. K. Chettiar, A. R. Davoyan, and N. Engheta, Hotspots from nonreciprocal surface waves, Opt. Lett. **39**, 1760 (2014).
[42] K. Tsakmakidis, L. Shen, S. Schulz, X. X. Zheng, J. Upham, X. Deng, H. Altug, A. Vakakis, and R. Boyd, Breaking Lorentz reciprocity to overcome the time-bandwidth limit in physics and engineering, Science **356**, 1260 (2017).
[43] S. A. Mann, D. L. Sounas, and A. Alu, Nonreciprocal cavities and the time-bandwidth limit, Optica **6**, 104 (2019).